

## Type-Dependent Impact of Aerosols on Precipitation Associated With Deep Convective Cloud Over East Asia

Xinlei Han<sup>1</sup>, Bin Zhao<sup>2</sup> , Yun Lin<sup>1</sup> , Qixiang Chen<sup>1</sup> , Hongrong Shi<sup>1</sup>, Zhe Jiang<sup>1</sup>, Xuehua Fan<sup>1</sup>, Jiandong Wang<sup>3</sup> , Kuo-Nan Liou<sup>1</sup>, and Yu Gu<sup>1</sup> 

<sup>1</sup>Joint Institute for Regional Earth System Science and Engineering and Department of Atmospheric and Oceanic Sciences, University of California, Los Angeles, CA, USA, <sup>2</sup>Pacific Northwest National Laboratory, Richland, WA, USA, <sup>3</sup>Department of Multiphase Chemistry, Max-Planck Institute for Chemistry, Mainz, Germany

**Key Points:**

- Dust and polluted continental aerosols enhance deep convective precipitation while elevated smoke suppresses it
- The aerosol invigoration effect is more significant for clouds with higher cloud base temperature
- Unlike terrestrial aerosols, marine aerosols first enhance and then inhibit precipitation with the increase of AOD

**Supporting Information:**

Supporting Information may be found in the online version of this article.

**Correspondence to:**

B. Zhao, Y. Gu and J. Wang,  
[zhaob1206@gmail.com](mailto:zhaob1206@gmail.com);  
[gu@atmos.ucla.edu](mailto:gu@atmos.ucla.edu);  
[jiandong.wang@mpic.de](mailto:jiandong.wang@mpic.de)

**Citation:**

Han, X., Zhao, B., Lin, Y., Chen, Q., Shi, H., Jiang, Z., et al. (2022). Type-dependent impact of aerosols on precipitation associated with deep convective cloud over East Asia. *Journal of Geophysical Research: Atmospheres*, 127, e2021JD036127. <https://doi.org/10.1029/2021JD036127>

Received 2 NOV 2021

Accepted 8 DEC 2021

**Abstract** Aerosol-cloud-precipitation interactions represent one of the most significant uncertainties in climate simulation and projection. In particular, the impact of aerosols on precipitation is highly uncertain due to limited and conflicting observational evidence. A major challenge is to distinguish the effects of different types of aerosols on precipitation associated with deep convective clouds, which produces most of the precipitation in East Asia. Here, we use 9-yr observations from multiple satellite-borne sensors and find that the occurrent frequency of heavy rain increases while that of light rain decreases with the increase of aerosol optical depth (AOD) for dust and polluted continental aerosol types. For average hourly precipitation amount, elevated smoke tends to suppress deep convective precipitation, while dust and polluted continental aerosols enhance precipitation mainly through the invigoration of deep convection. The invigoration effect is more significant for clouds with higher cloud base temperature (CBT), while no significant invigoration is observed when CBT is <12°C. A great contrast is found for the response of average hourly precipitation amount to aerosols over ocean and land. While the prevailing continental aerosol types other than smoke increase precipitation, the marine aerosols first enhance and then inhibit precipitation with the increase of AOD. Moreover, our analysis indicates that the above-mentioned enhancement and inhibition effects on precipitation are mainly caused by aerosols themselves, rather than by the covariation of meteorological factors. These observed relationships between different aerosol types and precipitation frequency and amount provide valuable constraints on the model forecasting of precipitation.

### 1. Introduction

The water circulation among atmosphere, land, surface, and ground water, that is, hydrological cycle, is crucial for life on Earth (Gleick, 1989; Levin & Cotton, 2009). Precipitation is one of the most important links in the hydrologic cycle, which determines the global water balance and the total amount of water resources in a region (Betts, 2007; Loaiciga et al., 1996; Morrissey & Graham, 1996). Given the manifested role of rainfall in the hydrologic cycle, the spatiotemporal redistribution of surface precipitation caused by the small changes in precipitating-related processes in clouds may largely affect climate and human society (Dolinar et al., 2016; Li et al., 2019; Pincus et al., 2008; Stephens & Kummerow, 2007; Wakimoto & Srivastava, 2017).

There is growing evidence that aerosols can alter total and extreme precipitation, which has been one of hot topics discussed in recent literature (Rosenfeld et al., 2014; Zhai et al., 2005). Among different types of clouds, deep convective clouds (DCCs) are found to be most abundant (Jiang et al., 2016), especially in East Asia. Therefore, understanding the response of precipitation associated with DCCs to aerosol effects is crucial for the weather forecast and climate projection.

Increasing aerosol concentrations can either inhibit or enhance the DCCs development, leading to various, even opposite effects on the precipitation occurrences or intensities (Fan et al., 2018; Khain et al., 2008; Koren et al., 2005; Lin et al., 2006; Niu & Li, 2011; Rosenfeld et al., 2005; Rosenfeld, 1999; Zhang et al., 2007). For example, Teller and Levin (2006) and Jiang et al. (2008) found that the precipitation rate (PR) associated with convective clouds decreases as aerosol loading increases, while others concluded that the PR tends to be enhanced by aerosol effect (Lin et al., 2006; Martins et al., 2009). A few studies did not find a consistent precipitation response to aerosol loading (Jones & Christopher, 2010). Many factors, for example, the analyzing location, time period, and their scales, as well as data source and techniques used, can influence aerosol effect evaluation, likely leading to the conflicting conclusions in previous studies (Koren et al., 2012). The underlying mechanism may be

linked to the aerosol effect on the microphysics and dynamics of DCCs. At present, the most popular hypothesis is the aerosol invigoration effect proposed by Rosenfeld et al. (2008), suggesting that aerosol particles acting as cloud condensation nuclei (CCN) can reduce collision-coalescence efficiency and thereby delay precipitation by forming small droplets, induce more condensation and freezing as the large amount of droplets are transported aloft, and eventually intensify cloud convection due to additional latent heat release. Many observational findings have support this viewpoint. Li et al. (2011) observed increased cloud top height (CTH) and cloud depth for warm-based DCCs with the increase of aerosols. Cold pool effect is also suggested to have considerable interfere the interaction between aerosol and DCCs associated with precipitation (Ackerman et al., 2004; Devara & Manoj, 2013; Grant & Heever, 2014; Jiang et al., 2016; Lebo & Morrison, 2014; Pincus & Baker, 1994; Sarangi et al., 2018; Storer & Heever, 2013; Tao et al., 2007). Recent observational evidence shows that precipitation changes as a typical boomerang shape when aerosol increases linearly (Guo et al., 2019; Koren et al., 2014), suggesting that aerosol net effect on precipitation tends to be saturated under polluted condition, which likely explains the “conflicting conclusions” found in previous studies and summarized above.

In addition, quantifying aerosol impacts on DCC properties by disentangling them from other environmental factors has been particularly challenging (Fan et al., 2016). Fan et al. (2009) found that aerosols can either suppress or intensify convection, depending on the intensity of vertical wind shear. Tao et al. (2007), on the other side, suggested that the response of rainfall from mature DCCs to aerosol loading varying with the environmental moisture and stability. For example, in humid environment the precipitation tends to be enhanced as aerosol loading increases, while it tends to decrease when the atmosphere is dry and unstable. The real problem may be that the main contributors to the discrepancy are not clear enough to predict exactly what the effect will be under what circumstances. Thus, the aerosol effects on precipitation should be understood under various thermodynamic and dynamic conditions, particularly for different humidity, wind shear, and atmospheric instability, as highlighted by previous studies.

As many factors can have impact on the relationship between aerosol and DCC precipitation, identifying major control variables is crucial for a quantitative evaluation of the net aerosol effect on DCC precipitation. Recently, some studies proposed that aerosol types have significant impact on cloud development. Zhao, Gu, et al. (2018) argued that the changes of ice cloud properties in response to different aerosol types are substantially different based on satellite data analysis. Jiang et al. (2018) also found aerosols could inhibit or invigorate development of DCC, depending on aerosol type. Because clouds are a prerequisite for precipitation formation, some research further investigated whether specific aerosol types have important effect on DCC precipitation. Based on analysis of multi-year satellite measurements, Huang et al. (2009) found that the decrease in precipitation in the West African Monsoon region can be attributed to aerosol emissions with various sources, including desert dust and biomass-burning smoke. Using satellite observations and reanalysis datasets Liu et al. (2019) found that the enhancement of the downstream precipitation over the Tibetan Plateau is because the cloud development over plateau is invigorated by the indirect effect of dust aerosols. The analysis on hourly precipitation observations combined with satellite measurements of aerosol and cloud properties by Zhou et al. (2020) revealed the role of aerosol types in changing heavy precipitation over the Beijing-Tianjin-Hebei region. Specifically, they found that absorbing aerosols like black carbon (BC) are responsible for the earlier times of start and peak of heavy precipitation, in contrast, scattering aerosols like sulfate can delay the start and make the precipitation event last longer.

However, as far as we know, previous studies have not systematically investigated the effects of different aerosol types on DCC precipitation from observational perspective. Studies regarding the aerosol effects on DCC precipitation over East Asia are especially limited and often show conflicting results (Fan et al., 2012; Li et al., 2019; Zhou et al., 2016), partly because the various aerosol types were seldom considered. In this study, we use 9-yr, multiple satellite measurements to explore the impacts of different aerosol types on precipitation frequency and average hourly precipitation amount. East Asia (i.e., 70°–135°E, 15°–55°N, see Figure S1), consistent with Zhao, Gu, et al. (2018), is selected as the studying area due to its vast territory and complex terrain, intensive anthropogenic emissions, and diverse aerosol types (Wang et al., 2014, 2017; Zhao et al., 2019; Zhao, Gu, et al., 2018; Zhao, Liou, et al., 2018).

## 2. Data and Methodology

### 2.1. Sources and Collocation of Satellite Retrievals

In our study, the collocated satellite retrievals of aerosol and cloud properties, and precipitation are mainly from “A-Train” series satellites (or satellite-borne sensors) including CALIOP (Cloud-Aerosol Lidar with Orthogonal Polarization) aboard Cloud-Aerosol Lidar and infrared Pathfinder Satellite Observations (CALIPSO), MODIS (Moderate Resolution Imaging Spectroradiometer) aboard Aqua, CloudSat, and from the Tropical Rainfall Measuring Mission (TRMM) for 2007–2015, as summarized in Table S1. Among these satellite retrievals, aerosol optical depth (AOD) comes from the MYDATM (Level 2, Collection 6.1) product, which is the MODIS/Aqua Joint Atmosphere product, a subset of datasets provided by the MODIS atmosphere team at a 10 km resolution for aerosols and 5 km resolution for clouds (either native 5 km cloud properties or a  $5 \times 5$  pixel sample of the 1 km cloud datasets). Column AOD is used as a proxy in this study for loadings of aerosols that interact with DCC. We use the 3-hr Realtime TRMM multi-satellite precipitation analysis dataset (3B42 RT) in our study with  $0.25^\circ \times 0.25^\circ$  and 3-hr resolutions. To better elaborate how and why aerosol related with precipitation associated with DCC, we further extracted the cloud top and base height from the 2B-CLDCLASS-LIDAR, version P1\_R05 product, a combined CloudSat-CALIOP product that has the detailed cloud three-dimensional structure information. Because cloud-base temperature is an important parameter in the activation of cloud drops (Johnson, 1980), we derive the cloud-base temperature corresponding to the cloud base height in 2B-CLDCLASS-LIDAR using the ERA5 reanalysis products (see below for a detailed introduction to ERA5).

In this study, we collocated the above satellite retrievals including aerosol and cloud properties, and precipitation measurements. First, we chose the profiles of CloudSat-CALIOP combined product (2B-CLDCLASS-LIDAR) at 1.7-km along track resolution as baselines, for its higher spatial resolution and more dedicated information on cloud vertical structure. Then, we matched aerosol, cloud and precipitation measurements from all sensors to the baselines. Given that AOD must be sampled from the area around centering the cloud but MODIS AOD is usually not available under cloudy condition, we searched AOD pixels from the  $10 \text{ km} \times 10 \text{ km}$  MYDATM product (level 2) within a 50 km radius from the CloudSat-CALIOP profiles to obtain sufficient AOD sample for average. According to Anderson et al. (2003), the spatial variation of lower-tropospheric aerosol extinction usually occurs on mesoscale (specifically, 40–400 km in horizontal ranges). In other words, the spatial variation of AOD below this scale is usually negligible (Anderson et al., 2003; Omar et al., 2013). This means that our spatially averaged AOD can represent the AOD at the location of the CloudSat-CALIOP profiles. We chose a single-layer cloud using the variable “cloud layer” information from 2B-CLDCLASS-LIDAR which has a 1.7 km along-track resolution and filtered the samples with valid quality assurance flags. The CALIOP data are matched to the CloudSat-CALIOP profiles to determine the aerosol types for each profile based on a method detailed in Section 2.2. Finally, the precipitation data were matched to the CloudSat-CALIOP profiles by selecting the closest time (within 3 hr) in the 3B42 RT/TRMM product and the corresponding  $0.25^\circ \times 0.25^\circ$  grid along with the CloudSat-CALIOP profiles.

To disentangle the meteorological influence from the observed relationship of aerosol and precipitation, a set of meteorological fields (Table S1) are extracted from the fifth generation European Centre for Medium-Range Weather Forecasts (ECMWF) atmospheric reanalysis of the global climate (ERA5). In our study, ERA5 datasets are collocated to corresponding CloudSat-CALIOP profiles by determining the nearest time in ERA5 according to the satellite overpassing time at the nearest ERA5  $0.25^\circ \times 0.25^\circ$  grids.

### 2.2. Determination of Cloud Types and Aerosol Types

In this study, we primarily used the 2B-CLDCLASS-LIDAR product to determine cloud types. The 2B-CLDCLASS-LIDAR combines CloudSat Cloud Profiling Radar (CPR) and CALIOP lidar measurements to categorize clouds into stratus, stratocumulus, cumulus (including cumulus congestus), nimbostratus, altocumulus, altostratus, deep convective (cumulonimbus), or high (cirrus and cirrostratus) clouds. By digesting the information of the full cloud vertical structure measured by lidar and radar, 2B-CLDCLASS-LIDAR can not only achieve overall cloud detection but also improve the accuracy of cloud classification. The combined measurements of CPR and CALIOP lidar can provide more reliable cloud phase identification as well (Deng et al., 2010) because CPR can better detect ice particles in mixed-phase clouds while lidar measurements are more sensitive in detecting liquid droplets. Moreover, the cloud phase in 2B-CLDCLASS-LIDAR is determined for each cloud layer, providing essential information for more accurate cloud type classification (Sassen et al., 2009; Sassen & Wang, 2008).

Aerosol type information is determined from the CALIOP aerosol data products, 05kmMLay (Level 2, version 4.1), released in November 2016, possessing substantial improved algorithms in classifying aerosol subtypes and selecting lidar ratio (Kim et al., 2018). The types of aerosols identified include dust, polluted dust, clean marine, clean continental aerosols, polluted continental aerosols, elevated smoke, and dusty marine aerosols in individual vertical layer. To our knowledge, the elevated smoke in China mainly comes from biomass burning, such as field burning of crop residues, as well as grassland and forest fires, with BC and organic compounds being the dominant compositions (Huang et al., 2016; Sun et al., 2016; Zhang et al., 2010). Before using the CALIOP aerosol types data, a rigorous assessment of CALIOP aerosol types is warranted by making use of ground-based aerosol property measurements from AERONET in the region. Therefore, we have evaluated the CALIOP aerosol classification over East Asia in Section S6 of the Supporting Information S1. The results show that CALIOP aerosol types are sufficiently reliable to support the statistical analyses in this study. It is worth noting that if the aerosol types are same for those layers identified as aerosol in all CALIOP profiles contained in a distance of 50-km from each CloudSat-CALIOP profile, the aerosol environment is assigned with that specific type to guarantee that the cases with mixing different types of aerosols are eliminated to the largest extent possible in the retrieval analysis (Zhao et al., 2019). The cases with different aerosol types for different CALIOP profiles or layers within a 50-km radius are grouped into “mixture of different types.”

### 3. Results and Discussion

#### 3.1. Overall Response of Precipitation Frequency to Different Types of Aerosols

Precipitation frequency, as referred to in this article, is defined as the number of samples with measurable precipitation over the total number of samples in each AOD bin. The measurable precipitation here means the rainfall measured by Precipitation Radar (PR) carried on the TRMM satellite. The minimum measurable PR detected by PR is 0.7 mm/hr with a range resolution and horizontal resolution of 250 m and 4 km, respectively (Fisher, 2004). Figure 1 shows the overall responses of precipitation frequencies of different intensity to different types of aerosols with the increase of AOD. According to the precipitation intensity classification standard from China Meteorological Administration (CMA), we use PR to classify precipitation into light rain ( $0 < PR < 1.5 \text{ mm hr}^{-1}$ ), moderate rain ( $1.5 \leq PR < 7 \text{ mm hr}^{-1}$ ), and heavy rain ( $PR \geq 7 \text{ mm hr}^{-1}$ ). PR is zero, which means that there is no precipitation. When all aerosol types are aggregated together (“all aerosols”), the total precipitation frequency for DCC system increases from 70% to 80% when AOD increases from 0.2 to 1.0. It also presents a significant trend that heavy rain occurs more frequent while the occurrence of light rain becomes less as AOD increases. This phenomenon is also obvious for the dust and polluted continental aerosol types. It is likely that these types of aerosols have the ability to invigorate DCCs (Koren et al., 2005) and furthermore enhance the occurrences of heavy precipitation. For other types of aerosols, the above trend is less significant.

For the elevated smoke aerosol, with the increase of AOD, the overall precipitation frequency increases (from 40% to 78%) while no heavy rain occurs when  $AOD > 0.6$ . It shows that the smoke aerosol may promote the occurrence of precipitation mainly by increasing the frequency of light and medium rain. Cloud microphysical processes and properties like the size distribution of droplet, warm and cold rain process, as well as CTH can vary with the changes in aerosol loading. It may be explained that when AOD is small, the aerosol invigoration effect is relatively obvious, while when AOD is large, the radiative effect is dominant and acts to inhibit the deep convection and heavy precipitation (Koren et al., 2008; Wang et al., 2018). For aerosols of clean and dusty marine, as well as a mixture of different types identified by CALIOP, there are no obvious signals for the responses of frequency to increasing aerosol loadings. These phenomena may be related to the limitation of sample number or the competition of the aerosol radiative effects and aerosol-cloud microphysical processes (Tao et al., 2012; Zamora & Kahn, 2020).

#### 3.2. Overall Response of Precipitation Intensity to Different Types of Aerosols

Figure 2 shows the relationships between MODIS AOD and TRMM average hourly precipitation amount and PR for different aerosol types. The average hourly precipitation amount is calculated as the average of precipitation amount within an hour for all valid samples (including samples with no precipitation) over the satellite transit time and the PR is the average of the samples with precipitation greater than zero. AOD is binned into three groups from low to high values. For AOD over land, it is divided into  $AOD < 0.2$ ,  $0.2 \leq AOD < 0.6$ , and

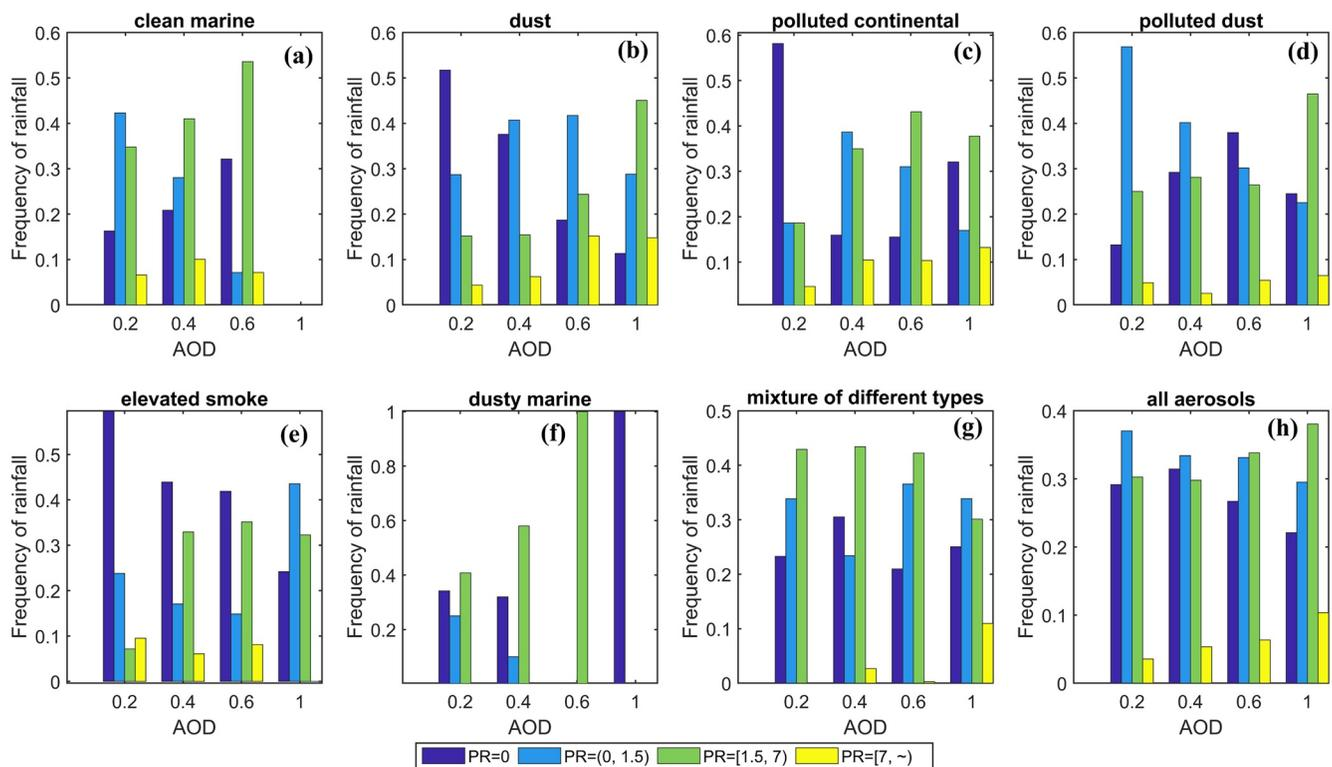


**Figure 1.** Responses of deep convective cloud (DCC) precipitation frequency to AOD for different aerosol types from 2007 to 2015. The precipitation intensity is divided according to the China Meteorological Administration precipitation intensity standard (GB/T 28592-2012) into four levels: no precipitation ( $PR = 0 \text{ mm hr}^{-1}$ ), light rain ( $0 \text{ mm hr}^{-1} < PR < 1.5 \text{ mm hr}^{-1}$ ), moderate rain ( $1.5 \text{ mm hr}^{-1} \leq PR < 7 \text{ mm hr}^{-1}$ ), and heavy rain ( $PR \geq 7 \text{ mm hr}^{-1}$ ). The total sample numbers of DCC are  $5.4 \times 10^3$ , among them,  $4.0 \times 10^2$  for clean marine,  $1.4 \times 10^3$  for dust,  $3.2 \times 10^2$  for polluted continental,  $1.1 \times 10^3$  for polluted dust,  $2.6 \times 10^2$  for elevated smoke,  $1.3 \times 10^2$  for dusty marine, and  $1.7 \times 10^3$  for mixture of different types of aerosols.

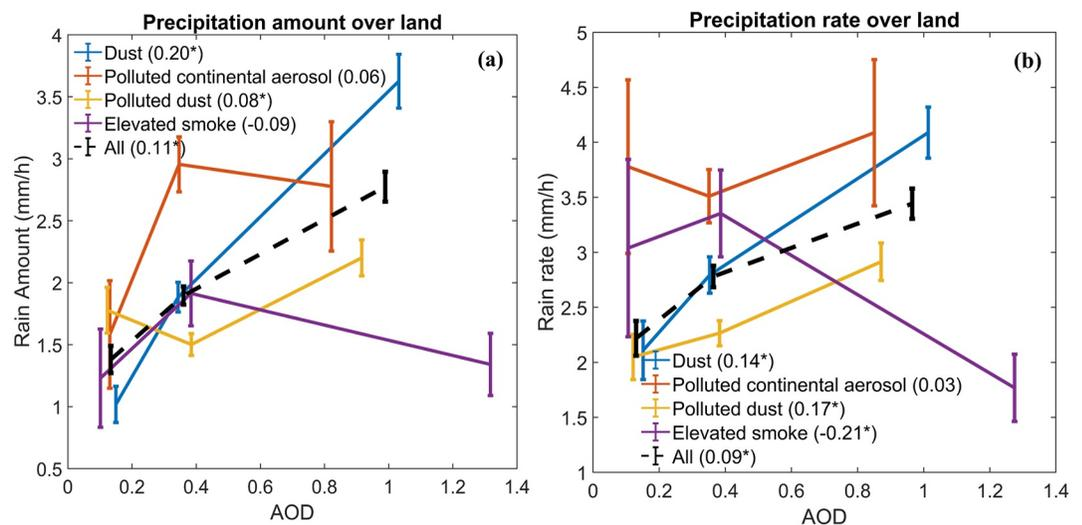


**Figure 2.** Response of DCC average hourly precipitation amount (a) and precipitation rate (b) to AOD for different aerosol types from 2007 to 2015. AOD is divided into 3 bins with increasing AOD values. For AOD over land, it is divided into  $AOD < 0.2$ ,  $0.2 \leq AOD < 0.6$ , and  $AOD \geq 0.6$ . The average values of AOD and precipitation of each bin are calculated. The vertical lines denote the standard errors ( $\sigma/\sqrt{N}$ ), where  $N$  is the sample number and  $\sigma$  is the standard deviation. The sample sizes of different types of aerosols are the same as these in Figure 1. The correlation coefficients of precipitation and AOD for different types of aerosol are calculated and presented in the legend. All the statistical results are tested by the Student's  $t$ -test and the value of correlation coefficient in the parentheses marked with \* is statistically significant ( $p < 0.01$ ).

AOD  $\geq 0.6$ . Then, the average values of AOD and average hourly precipitation amount and PR of each bin are calculated.

When all aerosol types are aggregated together, the overall response of hourly precipitation amount to aerosol loadings is a positive correlation in East Asia (shown by black dashed line in Figure 2a). With the increase of AOD, the hourly precipitation amount keeps increasing, from 1.4 to 2.6 mm hr<sup>-1</sup>; the correlation coefficient is 0.11, which is statistically significant as the Student's *t*-test shows  $p < 0.01$ . This phenomenon is likely to be explained by the abovementioned aerosol invigoration effect (Andreae et al., 2004; Rosenfeld et al., 2008). The responses of hourly precipitation amount to aerosol loadings from different types of aerosols have distinct features. It is obvious that in dust environment, the change of hourly precipitation amount with aerosol loadings presents the most significant positive trend. The total hourly precipitation amount increases from 1 to 3.5 mm hr<sup>-1</sup> when AOD increases from 0.2 to 1.1. For AOD  $< 0.5$ , the hourly precipitation amount has the largest increasing rate. The correlation coefficient of dust AOD loadings and hourly precipitation amount is 0.20, which is statistically significant. This is consistent with the result shown in Section 3.1 that the precipitation frequency increases with the increase of dust aerosol. These results together indicate that the increase of dust aerosol in East Asia may largely contribute to the rainfall enhancement in terms of both precipitation frequency and hourly precipitation amount. The response of hourly precipitation amount to the polluted dust aerosol is also a positive signal, but not as strong as dust type, showing a correlation coefficient of 0.08 and a *p*-value less than 0.01. For polluted continental aerosol, the response of hourly precipitation amount to AOD is generally positive but not statistically significant, with a correlation coefficient of 0.06. It is worth mentioning that the anthropogenic pollution sources are mainly in the areas with high humidity while the dust is mainly in dry areas with less rainfall, so once it rains in dry area, the magnitude of rainfall is likely to be more susceptible to aerosols. As for elevated smoke aerosol, on the contrary, it shows a first increasing (AOD  $< 0.5$ ) and then decreasing (AOD  $\geq 0.5$ ) trend of hourly precipitation amount with increasing AOD. The overall correlation coefficient between hourly precipitation amount and AOD is  $-0.09$ . This may be because the smoke aerosol is mainly an absorbing aerosol. When AOD is small, the smoke aerosol, like other types of aerosols, has the capability of serving as CCN to form clouds and further enhancing the precipitation due to the aerosol invigoration effect. However, when AOD is large, the atmospheric temperature profiles can be largely modulated by the atmospheric heating caused by absorbing aerosols like smoke and the resultant surface cooling. Also, semi-direct effect, that is, "burn out" of droplet, could be one possible cause. As mentioned in Section 3.1, this increases atmospheric stability and reduces moisture content because of evaporation, inhibiting the convection and precipitation (Ackerman et al., 2000; Koren et al., 2008).

The response of PR (shown in Figure 2b) to various aerosol types pretty much resembles that of average hourly precipitation amount (Figure 2a). For polluted continental aerosol, while the correlation coefficients are similar, the detailed patterns of the response differ to some extent. This may be related to a larger statistical error of this aerosol type due to a relatively small sample size. In general, the responses of DCC precipitation to different types of aerosols are reinforced by the similar pattern of hourly precipitation amount and PR.

The rainfall in East Asia mainly occurs in the wet season (between May and September). We show that, with the increase of AOD, the precipitation of different types of aerosols in wet season has the similar variations as those for the entire years, except that the hourly precipitation amount in wet season is larger than the yearly average value (Figure S2).

### 3.3. Responses Under Different Cloud Base Temperature (CBT)

According to the invigoration theory of Rosenfeld et al. (2008), invigoration occurs chiefly in warm-base convective clouds, because more latent heat can be generated in the warm-base convective clouds, which promotes the vertical development of cloud to a higher height. Many observational findings support this theory (Fan et al., 2009; Li et al., 2011; Niu & Li, 2011; Rosenfeld et al., 2008, 2014). Thus, CBT is a crucial controlling parameter for the aerosol invigoration effect. Therefore, we investigate the relationships between precipitation and AOD under different CBT conditions, as shown in Figures 3a and 3b). When the CBT is less than 12°C, the hourly precipitation amount and PR present no significant change with increasing AOD. However, when the CBT is greater than or equal to 12°C, both the hourly precipitation amount and PR gradually increase with the increase of AOD; the higher the CBT is, the more precipitation is promoted. There is also another possible reason that the clouds with warm CBT are lower than those with cold CBT and are thus more easily influenced by aerosols from surface.

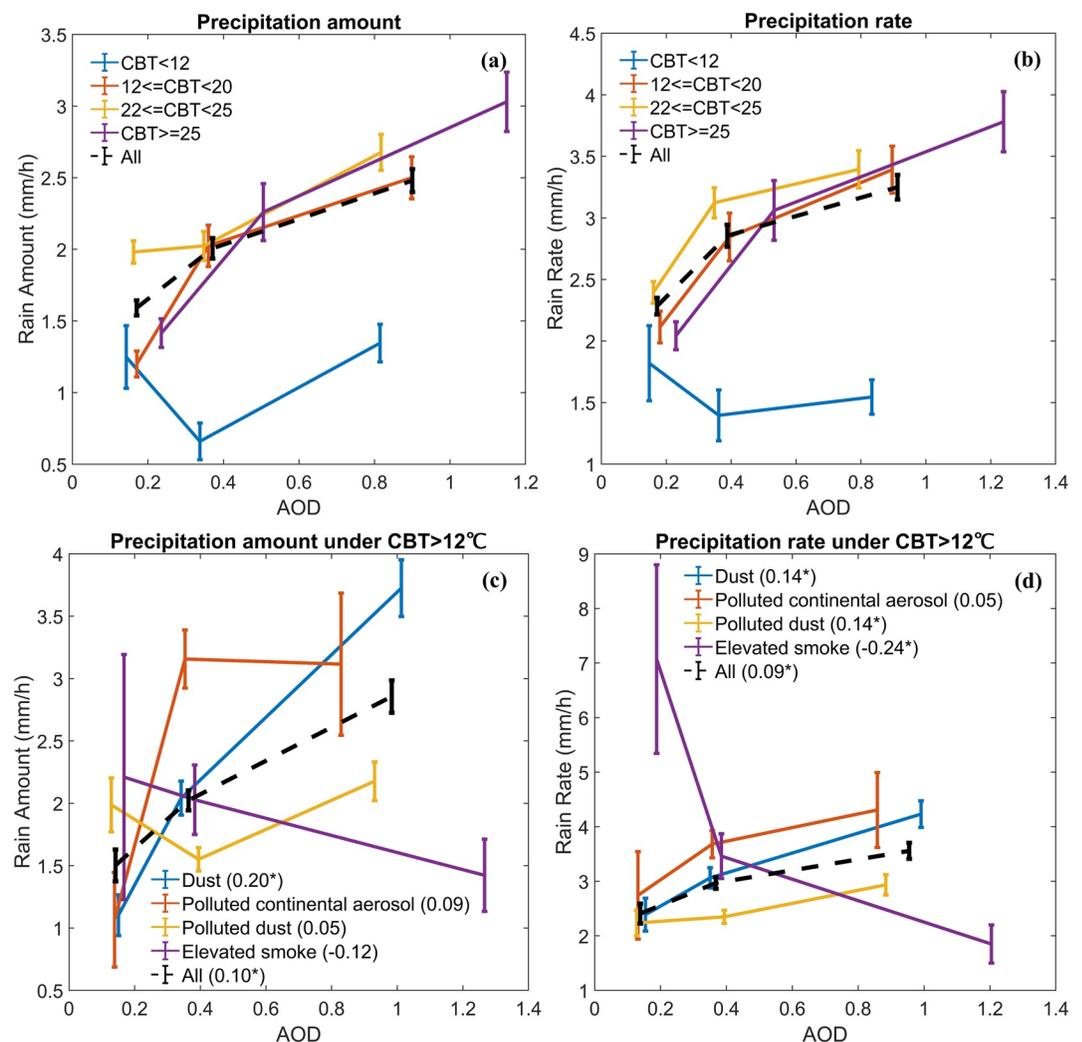


**Figure 3.** Response of (a) hourly precipitation amount and (b) precipitation rate to AOD under the condition of different CBT levels. (c) and (d) are the same as Figure 2, but for different aerosol types on the condition of CBT greater than 12°C.

To better explain the impacts of different aerosol types on the DCC precipitation system, we further explore whether precipitation has more significant variations with AOD loadings for clouds with warm bases. Figures 3c and 3d shows the response of DCC hourly precipitation amount and PR to AOD for different aerosol types on the condition of a warm base, that is CBT greater than 12°C. Compared with the results with all CBTs included (shown in Figure 2), the correlation of precipitation and AOD is more significant for polluted continental aerosol and elevated smoke aerosol, as indicated by larger correlation coefficients for these types of aerosols. Except for the smoke aerosol, all types of aerosols are positively correlated with PR.

### 3.4. Exclusion of Meteorological Factors

In studying the relationship between aerosol and precipitation, meteorological condition is still one possible cause that may lead to collaborative changes between the two. Some related studies have proved that meteorological conditions play a crucial rule in DCC precipitation. Tao et al. (2007) indicated the increase/decrease of precipitation with aerosols under wet/dry environment. Recently, Xiao et al. (2021) found that the impact of urbanization on precipitation, including anthropogenic aerosol effect, varies with different climate regions which are associated with distinct conditions of convective available potential energy (CAPE) and humidity. In order to test this possibility, we further analyze the relationship of hourly precipitation amount and aerosols under different meteorological parameters by using Pearson partial correlation analysis method. Partial correlation can

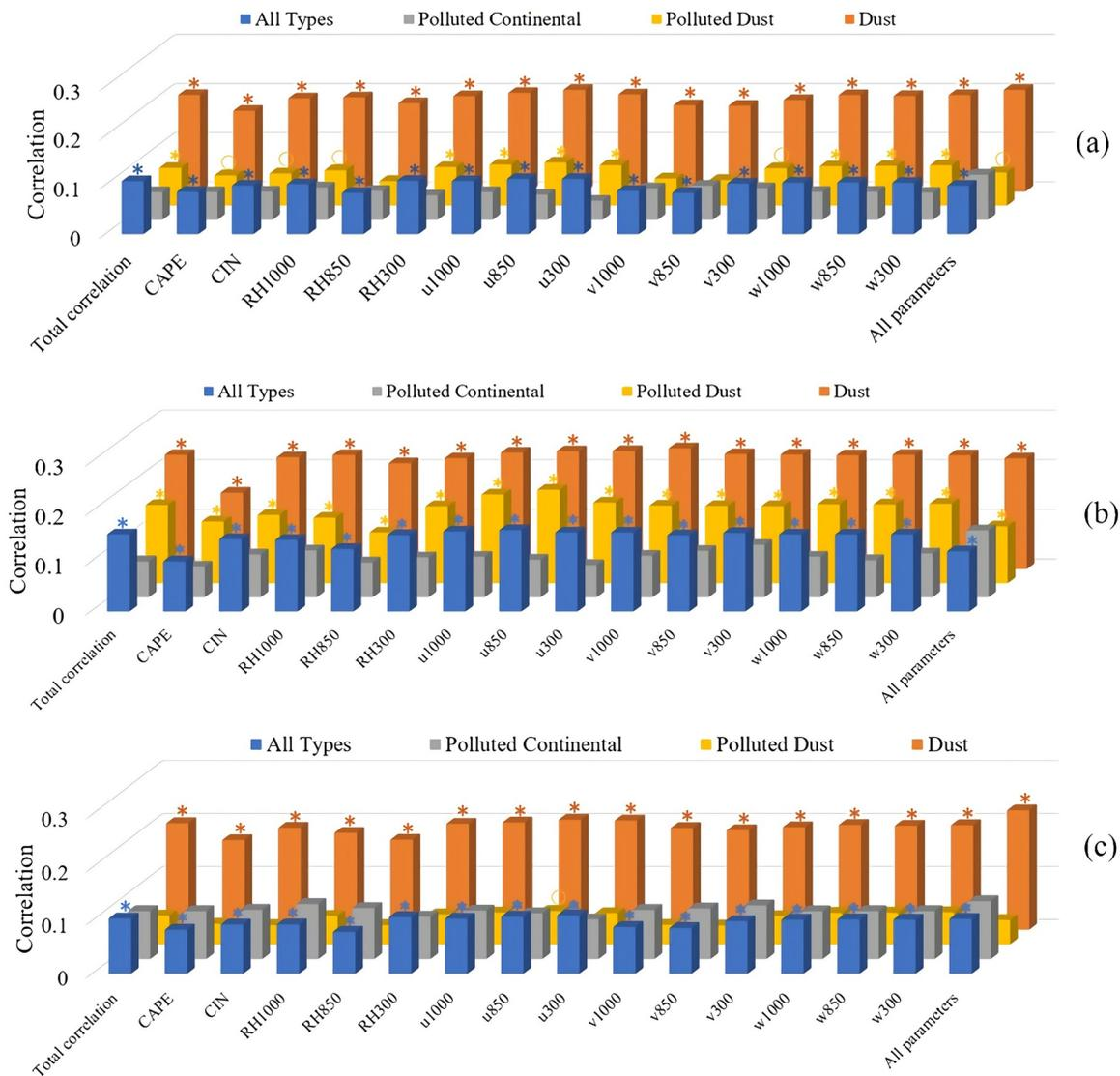


**Figure 4.** Pearson's total and partial correlations between AOD and hourly precipitation amount for all samples (a), only samples in wet season (b), and only samples with CBT > 12°C (c). The leftmost and rightmost columns denote the total correlation and partial correlations with the influence of all the 14 meteorological parameters simultaneously removed, respectively. The remaining columns denote partial correlations with the meteorological effect removed individually. The correlations that are statistically significant at the 0.01 level on the basis of the Student *t*-test are marked with \* symbol and those with statistical significance at the 0.05 level are marked with o symbol.

be used to measure the correlation between two variables (hourly precipitation amount and AOD) without the interference of other possible influential variables (e.g., meteorological factors in this study; Zhao, Gu et al., 2018). The latest reanalysis data, ERA5, is used to statistically analyze the impact of meteorological fields, including relative humidity, wind speed, CAPE, and convective inhibition, on the relationship between AOD and precipitation. Figure 4 shows the total correlations and the partial correlations between AOD of different aerosol types and hourly precipitation amount with the influence of 14 meteorological parameters removed either individually or simultaneously. Here, because the effect of elevated smoke on the correlation of precipitation and aerosol is not monotonous, it is not appropriate to employ the Pearson partial correlation analysis. Figures 4a–4c show the results for all samples for 2007–2015, samples in wet season (May–September) only, and samples with CBT greater than 12°C only, respectively. It can be seen that for each type of aerosol, the sign of all the partial correlations without the effects of any or all meteorological parameters is consistent with the counterparts of total correlation, and the relative difference from total to all partial correlations is less than 40%, suggesting that the most of the correlations ( $\geq 60\%$ ) are due to aerosols themselves. As the meteorological factors have limited effect

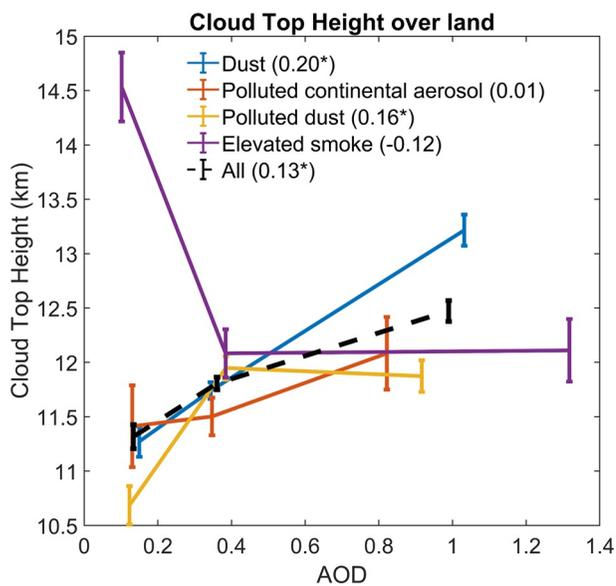


**Figure 5.** Changes in CTH with the increase in AOD of different aerosol types over land. The correlation coefficient of CTH and AOD for different types of aerosol is calculated and presented in the legend. All the statistical results are tested by the Student's *t*-test and the value of correlation coefficient marked with \* is statistically significant ( $p < 0.01$ ). The error bars are derived in the same way as in Figure 2.

For polluted continental aerosol and polluted dust aerosol, the CTH also shows a positive correlation with the increase AOD, but not as significant as that for the dust aerosol. This result confirms the invigoration effect of these types of aerosols and therefore the positive trend of precipitation with the increasing AOD presented earlier is well explained. This means that, dust, polluted continental and polluted dust aerosols indeed have the potential to enhance the DCCs precipitation through the processes of aerosol invigoration effect. For smoke aerosol, the CTH generally decreases with the increase of AOD, different from the results for other aerosol types. This is most likely due to a strong absorption characteristic of the smoke aerosol, which makes the cloud droplets evaporate, changes the cloud temperature profile, inhibits the development of convection (Ackerman et al., 2000; Koren et al., 2008). This result well explains the phenomenon that the precipitation is suppressed in the case of high smoke.

### 3.6. Comparison With Responses of Precipitation Over Ocean

Figure 6 shows the responses of hourly precipitation amount and PR to AOD of different aerosol types over ocean. There is a big difference in aerosol impact on the precipitation of DCCs between over land (Figure 2) and over ocean. Our observations show that terrestrial aerosols except for the smoke aerosol contribute to the increase of hourly precipitation amount and PR. However, response of precipitation to aerosols over ocean presents first an increasing and then a decreasing trend. Marine aerosols are further subdivided into the clean marine aerosol and the dusty marine aerosol. The response of precipitation to aerosol loadings for the clean marine aerosol is consistent with the overall marine aerosol, with the first increasing and then decreasing trend. When the AOD is low ( $AOD < 0.25$ ), the effect of the dusty marine aerosol on hourly precipitation amount and PR is similar to that of the clean marine aerosol, while after  $AOD > 0.25$ , the increasing trend in hourly precipitation amount and PR retains for dusty marine aerosol, different from the clean marine aerosol. This may be due to that dust dominates the dusty marine aerosol when  $AOD > 0.25$ , and dusty marine aerosol largely manifests the dust characteristics of enhancing precipitation.

Regarding the precipitation mechanism on ocean and land, Rosenfeld et al. (2008) suggested that the invigorating effect of aerosol on DCCs is different between land and ocean. With the increase of CCN, more buoyancy is needed to promote the development of cloud. When the energy is not enough to support the development of

on the correlations for dust, polluted continental and polluted dust aerosols, it is speculated that meteorological conditions also have limited impact on the correlation for smoke aerosols. Moreover, the correlation coefficients of precipitation and aerosols have been improved under the condition of wet seasons or the CBT greater than  $12^{\circ}\text{C}$ , which indicates that wet seasons or warm base cloud is more conducive to precipitation with the increase in AOD of the aerosol types considered here.

Besides, we have also ruled out the possible dependence of observed AOD-precipitation correlations on meteorological regimes associated with different seasons or regions. For details, see Sections 4 and 5, Figures S3 and S4; Table S2 of the Supporting Information S1.

### 3.5. CTH for Different Types of Aerosols

In the previous sections we proposed that the observed aerosol effect on precipitation is probably attributed to the invigoration (for most aerosol types) or inhibition (for a high loading of smoke aerosol) of convection. In order to verify this hypothesis, one direct way is to examine the changes in CTH, which is an indicator of convective strength.

In this study, we use the CTH derived from 2B-CLDCLASS-LIDAR of CloudSat-CALIPSO products to characterize the changes of cloud top characteristics (Figure 5) and find that the changes of CTH with AOD of different aerosol types show great differences. For dust aerosol on land, the CTH increases significantly with the increase of AOD. Compared with other types of aerosols, invigoration is the most obvious under dust environment.

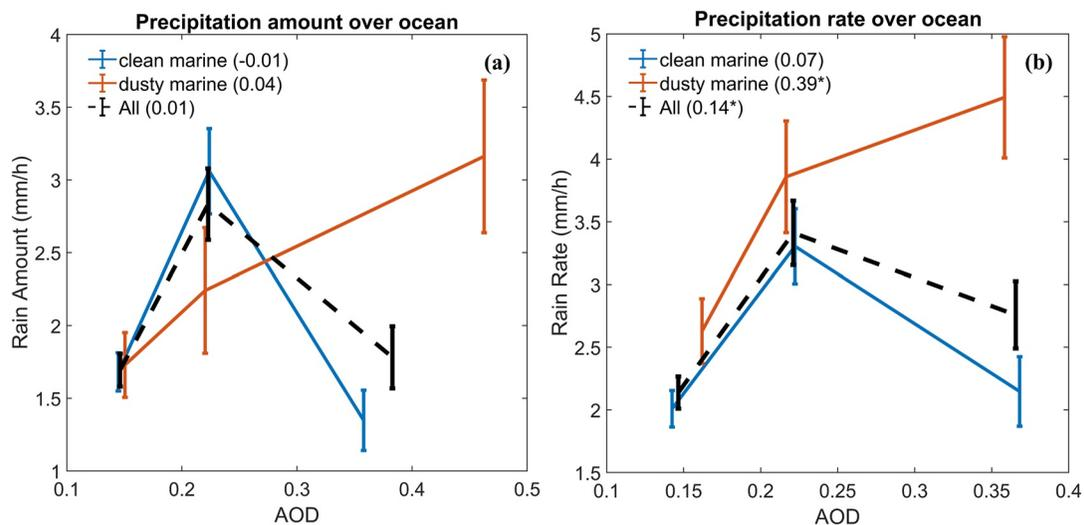


Figure 6. The same as Figure 2, but for the ocean.

convective cloud, it will settle down to form rainfall. In other words, aerosol first enhances and then inhibits deep convective precipitation with the increase of aerosol loading. Marine clouds with low CCN concentration rain quickly and reach the tipping point earlier, while more polluted terrestrial clouds are still in the invigoration stage. Rosenfeld et al. (2005) and Khain et al. (2005) also investigated the mechanisms of the aerosol impact on the dynamics and microphysics of DCCs using a 2D cloud model. They found that raindrops form efficiently as they fall through updrafts in cloud when maritime aerosols are present. However, continental-type aerosols lead to clouds developed with larger vertical velocities and at higher levels, accompanying with heavy precipitation.

#### 4. Conclusions and Implications

In this study, we analyze the impacts of different aerosol types on the precipitation frequency, hourly precipitation amount, and PR associated with DCCs by using multi-source satellite observation data. The results show that heavy rain becomes more frequent while light rain occurs less as AOD increases for dust and polluted continental aerosol types. At the same time, with the increase of AOD, dust aerosol and polluted continental aerosol, polluted dust aerosol can enhance hourly precipitation amount and PR, mainly due to the aerosol invigoration effect. However, for elevated smoke aerosol, increasing AOD enhances precipitation at small-to-moderate aerosol loadings (AOD < 0.5) but inhibits precipitation at larger aerosol loadings, which may be related to the aerosol radiative effect. Moreover, terrestrial and marine aerosols have different effects on hourly precipitation amount and PR, which may be due to different precipitation mechanisms on the ocean and land.

Reducing the uncertainties in aerosol-cloud-precipitation interaction is a tough task and how to isolate the aerosol effects on precipitation is challenging. One major challenge is to disentangle the effects of different aerosol types on different types of clouds (Jiang et al., 2018). Also, most previous studies about the impact of aerosol on precipitation are based on limited local or cases analysis (Fan et al., 2012; Li et al., 2019; Zhou et al., 2016), from which a long-term data analysis is lacking and the results remain controversial. In this study, we evaluate the influence of different types of aerosols on DCC precipitation, and the changes caused by atmospheric dynamics and/or thermodynamics are effectively minimized through the application of long-term satellite observations. The large samples are helpful to reveal a relative general phenomenon of the influence of aerosol types on DCCs precipitation over the region of interest. Also, it should be mentioned that the approach of using satellite data analysis proposed in this study could also be applied to other regions as well. More importantly, we provide comprehensive, solid observation-based evidence elaborating that the responses of DCC precipitation to aerosol loadings differ significantly in both sign and magnitude among different aerosol types. Although different responses have been reported in other studies for different types of aerosols, our study is concerned with more types than other individual studies. The results are helpful for the model evaluation of aerosol-cloud interaction and can be used as informative constraints on the future precipitation modeling.

Although this study proposes the probable mechanisms for the impact of different aerosol types on precipitation based on satellite-observed changes in CTH, in-depth modeling work is still needed to quantify the relative contributions of different mechanisms. Which physical processes are more significant or dominant for aerosol-induced changes in precipitation, for example, the radiative effects or the microphysical effects? The combination of observations and modeling will improve our understanding of the mechanism underlying the responses of clouds and precipitation to different aerosol types and their interplays.

## Data Availability Statement

The computation in this work was completed on the Cheyenne (<https://doi.org/10.5065/D6RX99HX>) cluster system of NCAR's Computational and Information Systems Laboratory, which is sponsored by the National Science Foundation. We have included all data that support the findings of this article in the main text and the Supporting Information S1.

## Acknowledgments

We acknowledge the support of the NASA ROSES TASNPP grant 80NSS-C18K0985, NSF grant AGS-2103820, and the NOAA grant NA19OAR4310243. Yu Gu acknowledges the support by (while serving at) the National Science Foundation. This work is also partly supported by the Joint Institute for Regional Earth System Science and Engineering in the University of California, Los Angeles. We would also like to thank Xiangao Xia for his helpful advice regarding this study.

## References

- Ackerman, A. S., Kirkpatrick, M. P., Stevens, D. E., & Toon, O. B. (2004). The impact of humidity above stratiform clouds on indirect aerosol climate forcing. *Nature*, *432*(7020), 1014–1017. <https://doi.org/10.1038/nature03174>
- Ackerman, A. S., Toon, O. B., Stevens, D. E., Heymsfield, A. J., Ramanathan, V., & Welton, E. J. (2000). Reduction of tropical cloudiness by soot. *Science*, *288*(5468), 1042–1047. <https://doi.org/10.1126/science.288.5468.1042>
- Anderson, T. L., Charlson, R. J., Winker, D. M., Ogren, J. A., & Holmén, K. (2003). Mesoscale variations of tropospheric aerosols. *Journal of the Atmospheric Sciences*, *60*(1), 119–136. [https://doi.org/10.1175/1520-0469\(2003\)060<0119:MVOTA>2.0.CO;2](https://doi.org/10.1175/1520-0469(2003)060<0119:MVOTA>2.0.CO;2)
- Andreae, M. O., Rosenfeld, D., Artaxo, P., Costa, A. A., Frank, G. P., Longo, K. M., & Silva-Dias, M. A. F. (2004). Smoking rain clouds over the Amazon. *Science*, *303*(5662), 1337–1342. <https://doi.org/10.1126/science.1092779>
- Betts, A. K. (2007). Coupling of water vapor convergence, clouds, precipitation, and land-surface processes. *Journal of Geophysical Research: Atmospheres*, *112*(10), 1–14. <https://doi.org/10.1029/2006JD008191>
- Deng, M., MacE, G. G., Wang, Z., & Okamoto, H. (2010). Tropical composition, cloud and climate coupling experiment validation for cirrus cloud profiling retrieval using cloudsat radar and CALIPSO lidar. *Journal of Geophysical Research*, *115*(17), 1–18. <https://doi.org/10.1029/2009JD013104>
- Devara, P. C. S., & Manoj, M. G. (2013). Aerosol-cloud-precipitation interactions: A challenging problem in regional environment and climate research. *Particology*, *11*(1), 25–33. <https://doi.org/10.1016/j.partic.2012.07.006>
- Dolinar, E. K., Dong, X., & Xi, B. (2016). Evaluation and intercomparison of clouds, precipitation, and radiation budgets in recent reanalyses using satellite-surface observations. *Climate Dynamics*, *46*(7–8), 2123–2144. <https://doi.org/10.1007/s00382-015-2693-z>
- Fan, J., Leung, L. R., Li, Z., Morrison, H., Chen, H., Zhou, Y., et al. (2012). Aerosol impacts on clouds and precipitation in eastern China: Results from bin and bulk microphysics. *Journal of Geophysical Research: Atmospheres*, *117*(2), 1. <https://doi.org/10.1029/2011JD016537>
- Fan, J., Rosenfeld, D., Zhang, Y., Giangrande, S. E., Li, Z., Machado, L. A. T., et al. (2018). Substantial convection and precipitation enhancements by ultrafine aerosol particles. *Science*, *418*, 411–418. <https://doi.org/10.1126/science.aan8461>
- Fan, J., Yuan, T., Comstock, J. M., Ghan, S., Khain, A., Leung, L. R., et al. (2009). Dominant role by vertical wind shear in regulating aerosol effects on deep convective clouds. *Journal of Geophysical Research*, *114*, 1–9. <https://doi.org/10.1029/2009JD012352>
- Fan, J. W., Wang, Y., Rosenfeld, D., & Liu, X. H. (2016). Review of aerosol–cloud interactions: Mechanisms, significance, and challenges. *Journal of Atmospheric Science*, *73*, 4221–4252.
- Fisher, B. L. (2004). Climatological validation of TRMM TMI and PR monthly rain products over Oklahoma. *Journal of Applied Meteorology*, *43*(3), 519–535. [https://doi.org/10.1175/1520-0450\(2004\)043<0519:cvotta>2.0.co;2](https://doi.org/10.1175/1520-0450(2004)043<0519:cvotta>2.0.co;2)
- Gleick, P. H. (1989). Climate change, hydrology, and water resources. *Reviews of Geophysics*, *27*(3), 329–344. <https://doi.org/10.1029/rg027i003p00329>
- Grant, L. D., & Heever, S. C. (2014). Cold pool and precipitation responses to aerosol loading: Modulation by dry layers. *Journal of the Atmospheric Sciences*, *72*, 1398–1408. <https://doi.org/10.1175/JAS-D-14-0260.1>
- Guo, J., Su, T., Chen, D., Wang, J., Li, Z., Lv, Y., et al. (2019). Declining summertime local-scale precipitation frequency over China and the United States, 1981–2012: The disparate roles of aerosols. *Geophysical Research Letters*, *46*(22), 13281–13289. <https://doi.org/10.1029/2019GL085442>
- Huang, J., Zhang, C., & Prospero, J. M. (2009). Large-scale effect of aerosols on precipitation in the West. *Quarterly Journal of the Royal Meteorological Society*, *594*, 581–594. <https://doi.org/10.1002/qj.391>
- Huang, X., Ding, A., Liu, L., Liu, Q., Ding, K., Niu, X., et al. (2016). Effects of aerosol-radiation interaction on precipitation during biomass-burning season in East China. *Atmospheric Chemistry and Physics*, *16*(15), 10063–10082. <https://doi.org/10.5194/acp-16-10063-2016>
- Jiang, J. H., Su, H., Huang, L., Wang, Y., Massie, S., Zhao, B., et al. (2018). Contrasting effects on deep convective clouds by different types of aerosols. *Nature Communications*, *9*(1). <https://doi.org/10.1038/s41467-018-06280-4>
- Jiang, J. H., Su, H., Schoeberl, M. R., Massie, S. T., Colarco, P., Platnick, S., & Livesey, N. J. (2008). Clean and polluted clouds: Relationships among pollution, ice clouds, and precipitation in South America. *Geophysical Research Letters*, *35*(14), 1–6. <https://doi.org/10.1029/2008GL034631>
- Jiang, M., Li, Z., Wan, B., & Cribb, M. (2016). Impact of aerosols on precipitation from deep convective clouds in eastern China. *Journal of Geophysical Research: Atmospheres*, *121*(16), 9607–9620. <https://doi.org/10.1002/2015JD024246>
- Johnson, D. B. (1980). The influence of cloud-base temperature and pressure on droplet concentration. *Journal of the Atmospheric Sciences*, *37*(9), 2079–2085. [https://doi.org/10.1175/1520-0469\(1980\)037<2079:TIOCBT>2.0.CO;2](https://doi.org/10.1175/1520-0469(1980)037<2079:TIOCBT>2.0.CO;2)
- Jones, T. A., & Christopher, S. A. (2010). Statistical properties of aerosol-cloud-precipitation interactions in South America. *Atmospheric Chemistry and Physics*, *10*(5), 2287–2305. <https://doi.org/10.5194/acp-10-2287-2010>
- Khain, A. P., Benmoshe, N., & Pokrovsky, A. (2008). Factors determining the impact of aerosols on surface precipitation from clouds: An attempt at classification. *Journal of the Atmospheric Sciences*, *65*, 1721–1748. <https://doi.org/10.1175/2007JAS2515.1>

- Khain, A. P., Rosenfeld, D., & Pokrovsky, A. (2005). Aerosol impact on the dynamics and microphysics of deep convective clouds. *Quarterly Journal of the Royal Meteorological Society*, *131*(611), 2639–2663. <https://doi.org/10.1256/qj.04.62>
- Kim, M. H., Omar, A. H., Tackett, J. L., Vaughan, M. A., Winker, D. M., Trepte, C. R., et al. (2018). The CALIPSO version 4 automated aerosol classification and lidar ratio selection algorithm. *Atmospheric Measurement Techniques*, *11*(11), 6107–6135. <https://doi.org/10.5194/amt-11-6107-2018>
- Koren, I., Altaratz, O., Remer, L. A., Feingold, G., Martins, J. V., & Heiblum, R. H. (2012). Aerosol-induced intensification of rain from the tropics to the mid-latitudes. *Nature Geoscience*, *5*, 3–122. <https://doi.org/10.1038/ngeo1364>
- Koren, I., Dagan, G., & Altaratz, O. (2014). From aerosol-limited to invigoration of warm convective clouds. *Science*, *344*(6188), 1143–1146. <https://doi.org/10.1126/science.1252595>
- Koren, I., Kaufman, Y. J., Rosenfeld, D., Remer, L. A., & Rudich, Y. (2005). Aerosol invigoration and restructuring of Atlantic convective clouds. *Geophysical Research Letters*, *32*(14), L14828. <https://doi.org/10.1029/2005gl023187>
- Koren, I., Vanderlei Martins, J., Remer, L. A., & Afargan, H. (2008). Smoke invigoration versus inhibition of clouds over the Amazon. *Science*, *321*(5891), 946–949. <https://doi.org/10.1126/science.1159185>
- Lebo, Z. J., & Morrison, H. (2014). Dynamical effects of aerosol perturbations on simulated idealized squall lines. *Monthly Weather Review*, *142*, 991–1009. <https://doi.org/10.1175/MWR-D-13-00156.1>
- Levin, Z., & Cotton, W. R. (2009). *Aerosol pollution impact on precipitation: A scientific review*. Springer. <https://doi.org/10.1007/978-1-4020-8690-8>
- Li, Z., Niu, F., Fan, J., Liu, Y., Rosenfeld, D., & Ding, Y. (2011). Long-term impacts of aerosols on the vertical development of clouds and precipitation. *Nature Geoscience*, *4*(12), 888–894. <https://doi.org/10.1038/ngeo1313>
- Li, Z., Wang, Y., Guo, J., Zhao, C., Cribb, M. C., Dong, X., et al. (2019). East Asian study of tropospheric aerosols and their impact on regional clouds, precipitation, and climate (EAST-AIRRPC). *Journal of Geophysical Research: Atmospheres*, *124*(23), 13026–13054. <https://doi.org/10.1029/2019JD030758>
- Lin, J. C., Matsui, T., Pielke, S. A., & Kummerow, C. (2006). Effects of biomass-burning-derived aerosols on precipitations and clouds in the Amazon basin: A satellite-based empirical study. *Journal of Geophysical Research: Atmospheres*, *111*(19), 1–14. <https://doi.org/10.1029/2005JD006884>
- Liu, Y., Zhu, Q., Huang, J., Hua, S., & Jia, R. (2019). Impact of dust-polluted convective clouds over the Tibetan Plateau on downstream precipitation. *Atmospheric Environment*, *209*, 67–77. <https://doi.org/10.1016/j.atmosenv.2019.04.001>
- Loaiciga, H. A., Valdes, J. B., Vogel, R., Garvey, J., & Schwarz, H. (1996). Global warming and the hydrologic cycle. *Journal of Hydrology*, *174*(1–2), 83–127. [https://doi.org/10.1016/0022-1694\(95\)02753-X](https://doi.org/10.1016/0022-1694(95)02753-X)
- Martins, J. A., Silva Dias, M. A. F., & Gonçalves, F. L. T. (2009). Impact of biomass burning aerosols on precipitation in the Amazon: A modeling case study. *Journal of Geophysical Research*, *114*(D2), 1–19. <https://doi.org/10.1029/2007jd009587>
- Morrissey, M. L., & Graham, N. E. (1996). Recent trends in rain gauge precipitation measurements from the tropical Pacific: Evidence for an enhanced hydrologic cycle. *Bulletin of the American Meteorological Society*, *77*(6), 1207–1219. [https://doi.org/10.1175/1520-0477\(1996\)077<1207:RTIRGP>2.0.CO;2](https://doi.org/10.1175/1520-0477(1996)077<1207:RTIRGP>2.0.CO;2)
- Niu, F., & Li, Z. (2011). Cloud invigoration and suppression by aerosols over the tropical region based on satellite observations. *Atmospheric Chemistry and Physics Discussions*, *11*(2), 5003–5017. <https://doi.org/10.5194/acpd-11-5003-2011>
- Omar, A. H., Winker, D. M., Tackett, J. L., Giles, D. M., Kar, J., Liu, Z., et al. (2013). CALIOP and AERONET aerosol optical depth comparisons: One size fits none. *Journal of Geophysical Research: Atmospheres*, *118*(10), 4748–4766. <https://doi.org/10.1002/jgrd.50330>
- Pincus, R., & Baker, M. B. (1994). Effect of precipitation on the albedo susceptibility of clouds in the marine boundary layer. *Nature*, *372*(6503), 250–252. <https://doi.org/10.1038/372250a0>
- Pincus, R., Batstone, C. P., Patrick Hofmann, R. J., Taylor, K. E., & Glecker, P. J. (2008). Evaluating the present-day simulation of clouds, precipitation, and radiation in climate models. *Journal of Geophysical Research: Atmospheres*, *113*(14), 1–10. <https://doi.org/10.1029/2007JD009334>
- Rosenfeld, D., Andreae, M., Asmi, A., Chin, M., Leeuw, G., Donovan, D. P., et al. (2014). Global observations of aerosol-cloud-precipitation-climate interactions. *Reviews of Geophysics*, *52*, 750–808. <https://doi.org/10.1002/2013RG000441>
- Rosenfeld, D., Lohmann, U., Raga, G. B., O'Dowd, C. D., Kulmala, M., Fuzzi, S., et al. (2008). Flood or drought: How do aerosols affect precipitation? *Science*, *321*(5894), 1309–1313. <https://doi.org/10.1126/science.1160606>
- Rosenfeld, D., Pokrovsky, A., & Ram, G. (2005). Aerosol impact on the dynamics and microphysics of deep convective clouds. *Quarterly Journal of the Royal Meteorological Society*, *131*, 2639–2663. <https://doi.org/10.1256/qj.04.62>
- Rosenfeld, D. (1999). TRMM observed first direct evidence of smoke from forest fires inhibiting rainfall. *Geophysical Research Letters*, *26*(20), 3105–3108.
- Sarangi, C., Kanawade, V. P., Tripathi, S. N., Thomas, A., & Ganguly, D. (2018). Aerosol-induced intensification of cooling effect of clouds during Indian summer monsoon. *Nature Communications*, *9*(1). <https://doi.org/10.1038/s41467-018-06015-5>
- Sassen, K., & Wang, Z. (2008). Classifying clouds around the globe with the CloudSat radar: 1-year of results. *Geophysical Research Letters*, *35*(4), 1–5. <https://doi.org/10.1029/2007GL032591>
- Sassen, K., Wang, Z., & Liu, D. (2009). Global distribution of cirrus clouds from CloudSat/cloud-aerosol lidar and infrared pathfinder satellite observations (CALIPSO) measurements. *Journal of Geophysical Research: Atmospheres*, *114*(8), 1–12. <https://doi.org/10.1029/2008JD009972>
- Stephens, G. L., & Kummerow, C. D. (2007). The remote sensing of clouds and precipitation from space: A review. *Journal of the Atmospheric Sciences*, *64*(11), 3742–3765. <https://doi.org/10.1175/2006JAS2375.1>
- Storer, R. L., & Heever, S. C. (2013). Microphysical processes evident in aerosol forcing of tropical deep convective clouds. *Journal of the Atmospheric Sciences*, *70*, 430–446. <https://doi.org/10.1175/JAS-D-12-076.1>
- Sun, Y., Jiang, Q., Xu, Y., Ma, Y., Zhang, Y., Liu, X., et al. (2016). Aerosol characterization over the North China Plain: Haze life cycle and biomass burning impacts in summer. *Journal of Geophysical Research: Atmospheres*, *121*, 2508–2521. <https://doi.org/10.1002/2015JD024261>
- Tao, W. K., Chen, J. P., Li, Z., Wang, C., & Zhang, C. (2012). Impact of aerosols on convective clouds and precipitation. *Reviews of Geophysics*, *50*(2). <https://doi.org/10.1029/2011RG000369>
- Tao, W. K., Li, X., Khain, A., Matsui, T., Lang, S., & Simpson, J. (2007). Role of atmospheric aerosol concentration on deep convective precipitation: Cloud-resolving model simulations. *Journal of Geophysical Research*, *112*, D24S18. <https://doi.org/10.1029/2007JD008728>
- Teller, A., & Levin, Z. (2006). The effects of aerosols on precipitation and dimensions of subtropical clouds: A sensitivity study using a numerical cloud model. *Atmospheric Chemistry and Physics*, *6*, 67–80. <https://doi.org/10.5194/acp-6-67-2006>
- Wakimoto, R. M., & Srivastava, R. (2017). *Radar and atmospheric science: A collection of essays in honor of David atlas* (Vol. 98). Bulletin of the American Meteorological Society. <https://doi.org/10.1175/BAMS-D-15-00130.1>
- Wang, J., Zhao, B., Wang, S., Yang, F., Xing, J., Morawska, L., et al. (2017). Particulate matter pollution over China and the effects of control policies. *The Science of the Total Environment*, *584*–585, 426–447. <https://doi.org/10.1016/j.scitotenv.2017.01.027>

- Wang, Q., Li, Z., Guo, J., Zhao, C., & Cribb, M. (2018). The climate impact of aerosols on the lightning flash rate: Is it detectable from long-term measurements? *Atmospheric Chemistry and Physics*, *18*(17), 12797–12816. <https://doi.org/10.5194/acp-18-12797-2018>
- Wang, S. X., Zhao, B., Cai, S. Y., Klimont, Z., Nielsen, C. P., Morikawa, T., et al. (2014). Emission trends and mitigation options for air pollutants in East Asia. *Atmospheric Chemistry and Physics*, *14*(13), 6571–6603. <https://doi.org/10.5194/acp-14-6571-2014>
- Xiao, F., Zhu, B., & Zhu, T. (2021). Inconsistent urbanization effects on summer precipitation over the typical climate regions in central and eastern China. *Theoretical and Applied Climatology*, *143*(1–2), 73–85. <https://doi.org/10.1007/s00704-020-03404-z>
- Zamora, L. M., & Kahn, R. A. (2020). Saharan dust aerosols change deep convective cloud prevalence, possibly by Inhibiting Marine New Particle formation. *Journal of Climate*, *33*(21), 9467–9480. <https://doi.org/10.1175/JCLI-D-20-0083.1>
- Zhai, P., Zhang, X., Wan, H., & Pan, X. (2005). Trends in total precipitation and frequency of daily precipitation extremes over China. *Journal of Climate*, *18*, 1096–1108. <https://doi.org/10.1175/jcli-3318.1>
- Zhang, R., Li, G., Fan, J., Wu, D. L., & Molina, M. J. (2007). Intensification of Pacific storm track linked to Asian pollution. *Proceedings of the National Academy of Sciences of the United States of America*, *104*(18), 5295–5299. <https://doi.org/10.1073/pnas.0700618104>
- Zhang, Z., Engling, G., Lin, C. Y., Chou, C. C. K., Lung, S. C. C., Chang, S. Y., et al. (2010). Chemical speciation, transport and contribution of biomass burning smoke to ambient aerosol in Guangzhou, a mega city of China. *Atmospheric Environment*, *44*(26), 3187–3195. <https://doi.org/10.1016/j.atmosenv.2010.05.024>
- Zhao, B., Gu, Y., Liou, K. N., Wang, Y., Liu, X., Huang, L., et al. (2018). Type-dependent responses of ice cloud properties to aerosols from satellite retrievals. *Geophysical Research Letters*, *45*(7), 3297–3306. <https://doi.org/10.1002/2018GL077261>
- Zhao, B., Liou, K., Gu, Y., Jiang, J. H., Li, Q., Fu, R., et al. (2018). Impact of aerosols on ice crystal size. *Atmospheric Chemistry and Physics*, *2*(18), 1065–1078. <https://doi.org/10.5194/acp-18-1065-2018>
- Zhao, B., Wang, Y., Gu, Y., Liou, K. N., Jiang, J. H., Fan, J., et al. (2019). Ice nucleation by aerosols from anthropogenic pollution. *Nature Geoscience*, *12*(8), 602–607. <https://doi.org/10.1038/s41561-019-0389-4>
- Zhou, C., Zhang, X., Gong, S., Wang, Y., & Xue, M. (2016). Improving aerosol interaction with clouds and precipitation in a regional chemical weather modeling system. *Atmospheric Chemistry and Physics*, *16*(1), 145–160. <https://doi.org/10.5194/acp-16-145-2016>
- Zhou, S., Yang, J., Wang, W. C., Zhao, C., Gong, D., & Shi, P. (2020). An observational study of the effects of aerosols on diurnal variation of heavy rainfall and associated clouds over Beijing-Tianjin-Hebei. *Atmospheric Chemistry and Physics*, *20*(9), 5211–5229. <https://doi.org/10.5194/acp-20-5211-2020>

## References From the Supporting Information

- Mielonen, T., Arola, A., Komppula, M., Kukkonen, J., Koskinen, J., De Leeuw, G., & Lehtinen, K. E. J. (2009). Comparison of CALIOP level 2 aerosol subtypes to aerosol types derived from AERONET inversion data. *Geophysical Research Letters*, *36*(18), 1–5. <https://doi.org/10.1029/2009GL039609>
- Omar, A. H., Winker, D. M., Vaughan, M. A., Hu, Y., Trepte, C. R., Ferrare, R. A., et al. (2009). The CALIPSO automated aerosol classification and lidar ratio selection algorithm. *Journal of Atmospheric and Oceanic Technology*, *26*(10), 1994–2014. <https://doi.org/10.1175/2009jtecha1231.1>
- Tesche, M., Wandinger, U., Ansmann, A., Althausen, D., Müller, D., & Omar, A. H. (2013). Ground-based validation of CALIPSO observations of dust and smoke in the Cape Verde region. *Journal of Geophysical Research: Atmospheres*, *118*(7), 2889–2902. <https://doi.org/10.1002/jgrd.50248>
- Wu, Y., Cordero, L., Gross, B., Moshary, F., & Ahmed, S. (2014). Assessment of CALIPSO attenuated backscatter and aerosol retrievals with a combined ground-based multi-wavelength lidar and sunphotometer measurement. *Atmospheric Environment*, *84*, 44–53. <https://doi.org/10.1016/j.atmosenv.2013.11.016>